Magnetocrystalline anisotropy of La- and Co-substituted M-type strontium ferrites: Role of Co^{2+} and Fe^{2+}

Hiroaki Ueda,* Yasuaki Tanioku, Chishiro Michioka, and Kazuyoshi Yoshimura
Department of Chemistry, Graduate School of Science, Kyoto University, Kitashirakawa Oiwake-cho, Sakyo-ku, Kyoto 606-8502, Japan
(Received 1 March 2017; revised manuscript received 4 May 2017; published 16 June 2017)

We have systematically investigated the magnetic properties of La- and Co-substituted $SrFe_{12}O_{19}$ using single crystals. By utilizing the traveling solvent floating zone technique, we have grown single crystals over a wide range of substitution content, and examined their saturation moments and magnetocrystalline anisotropy. With increasing content of La and Co, the saturation moment at 300 K monotonically increases. The increment of magnetocrystalline anisotropy is almost proportional to the content of Co. In addition, further La substitution also enhances magnetocrystalline anisotropy, which demonstrates that Fe^{2+} plays an important role to enhance magnetocrystalline anisotropy. We have analyzed magnetocrystalline anisotropy energy as a function of substitution content, and elucidate the effects of Co^{2+} and Fe^{2+}.

DOI: 10.1103/PhysRevB.95.224421

I. INTRODUCTION

The hexagonal ferrites that have the magnetoplumbite (*M*-type) structure are important materials for permanent magnets. Since the discovery of *M*-type hexaferrites [1], they have attracted much attention [2]. Because of their competitive price and easy preparation in comparison with other magnetic materials, they have been extensively used in applications such as electronics, household appliances and communications. They are ferrimagnets with high coercivity, which originates from high magnetocrystalline anisotropy with an easy magnetization axis. Many attempts have been made to improve their magnetic properties [3,4]. Among them, the latest breakthrough is based on partial substitutions with La and Co, which are expressed as a $Sr_{1-x}La_xFe_{12-x}Co_xO_{19}$ chemical formula [5].

All the Fe ions in the strontium hexaferrite $SrFe_{12}O_{19}$ are trivalent and have a high spin electron configuration of d^5, which has a vanishing orbital momentum. In the substituted materials $Sr_{1-x}La_xFe_{12-x}Co_xO_{19}$, a fraction of Fe^{3+} is substituted by Co^{2+}, and the same amount of Sr^{2+} is substituted by La^{3+} for charge compensation. The improvement of magnetic properties in this system is reported to be caused by drastic increment of the magnetocrystalline anisotropy field [5]. The origin of the enhancement of magnetocrystalline anisotropy field is thought to be not due to La^{3+} but due to Co^{2+}, which has a residual orbital momentum. However, in spite of many studies on La- and Co-substituted samples, the details remain unclear.

The crystal structure of *M*-type hexaferrite is regarded as alternate stacking of S and R layers [6] and have crystallographically inequivalent five Fe sites, which include tetrahedral, octahedral, and trigonal-bipyramid sites. This complicated crystal structure makes it difficult to determine the site where Co is substituted [7–10]. In addition, almost all the previous studies of these substances were conducted using polycrystalline samples, and their results include the effect of orientations, grain size and grain boundaries. To remove these extrinsic effects, it is required to study using single crystals, though there are only a few reports dealing with single-crystal growth [11–13].

In this paper, we report crystal growth, compositional analysis, and magnetic properties of single crystals of $Sr_{1-x}La_xFe_{12-y}Co_yO_{19}$, and discuss the origin of the enhancement of magnetocrystalline anisotropy in this system. In our single crystals, the content of La is greater than or equal to that of Co, indicating presence of Fe^{2+}. We measured saturation magnetizations and anisotropy fields, both of which increase with substitution content at 300 K. In addition, the magnetocrystalline anisotropy energy is analyzed as a function of the contents of Co^{2+} and Fe^{2+} to elucidate the origin of magnetocrystalline anisotropy.

II. EXPERIMENTS

The single-crystal samples of La- and Co-substituted strontium hexaferrites were grown using the traveling solvent floating zone (TSFZ) technique in an infrared radiation furnace equipped with two ellipsoidal mirrors (SC-E15HD, Cannon machinery). Stoichiometric mixtures of $SrCO_3$, $LaFeO_3$, Fe_2O_3, and CoO were pressed into cylindrical rods, and these rods were sintered. Mixtures of above materials were used as fluxes. A typical chemical composition of these fluxes is $(La,Sr)(Fe,Co)_2O_4$. Crystals were grown at a rate of 1 mm/h under a 10 atm O_2 atmosphere. The typical size of the obtained single crystals is 4 mm in diameter and 60 mm in length. Powder x-ray diffraction measurements were conducted using a diffractometer with a Cu-Kα source (Miniflex 600, Rigaku). We carried out compositional analysis of the single crystals using scanning electron microscopy/wavelength dispersive x-ray (SEM-WDX) analysis (INCA wave 500, Oxford Instruments, attached to SEM S-3500H, Hitachi) and inductively coupled plasma atomic emission spectrometry (ICP-AES) (JY138KH, Horiba Ltd.). Magnetization measurements were conducted at high temperatures using a handmade magnetic balance to determine the Curie temperatures. The magnetization at low temperatures was measured using a SQUID magnetometer (MPMS, Quantum Design) in the Research Center for Low Temperature and Materials Sciences, Kyoto University. Before the measurements, the crystals were cut into rectangular rods

*weda@kuchem.kyoto-u.ac.jp

with a typical size of $0.5 \times 0.5 \times 2$ mm^3 in order to reduce the demagnetization factor, which was calculated using a reported formula [14]. The samples were fixed at the center of a brass rod that was precisely positioned at the center of the detection coil.

III. RESULTS AND DISCUSSION

We had already succeeded in growing single crystals of $SrFe_{12}O_{19}$ using TSFZ [15]. On the basis of the charge compensation model, we tried to grow single crystals that have chemical compositions of $Sr_{1-x}La_xFe_{12-x}Co_xO_{19}$. We found that high oxygen pressure is preferable to grow single crystals in this system, and hence the crystals were grown under a 10 atm O_2 atmosphere. For the samples with $x \leqslant 0.4$, we succeeded in obtaining single crystals, which indicate that their chemical compositions are the same as the nominal compositions. However, for the samples with $x \geqslant 0.5$, the obtained crystals contain impurities, which are observed as tiny crystals sparsely scattered on cleaved surfaces as shown in the left inset of Fig. 1. Diffraction and magnetization measurements revealed that the main impurity is a spinel compound. The formation of impurities indicates that the chemical composition of M-phases in the samples with $x \geqslant 0.5$ are different from nominal compositions.

For $x \leqslant 0.4$, we conducted ICP measurements, which gives the averaged chemical compositions of bulk crystals. In order to determine the chemical composition of M phase in a sample that contains impurities, we have to remove the contribution of impurities, which are scattered in the crystals. For this purpose, we carried out an SEM-WDX analysis of the M phases on cleaved surfaces of the sample with $0.1 \leqslant x \leqslant 0.7$. These results are summarized in Fig. 1. For $x \leqslant 0.4$, the results of both WDX and ICP are in good agreement with

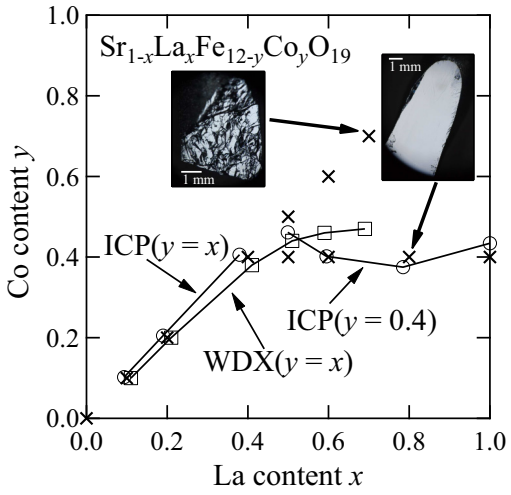

FIG. 1. Nominal and measured compositions of single-crystal samples of $Sr_{1-x}La_xFe_{12-y}Co_yO_{19}$. Crosses indicate nominal compositions, which is the same value as that of the starting materials. Squares and circles indicate compositions obtained using WDX and those using ICP, respectively. The insets are pictures of cleaved surfaces of obtained single crystals with nominal compositions of $(x, y) = (0.7, 0.7)$ and $(0.8, 0.4)$.

nominal compositions. However, for $x \geqslant 0.5$, the Co contents obtained using WDX are obviously less than those of nominal compositions, though La contents are almost the same as those of nominal compositions. These results suggest that Co substitution is limited to $x \lesssim 0.4$ under the condition that we applied. This value of substitution limit $x = 0.4$ is almost the same as in a previous report [5] on polycrystalline samples synthesized in air, which may be a coincidence. For the sample with $x = 0.4$, the equilibrium O_2 partial pressure is thought to be approximately 20% at 1200 °C, the synthesis temperature of the polycrystalline sample. A single crystal with the same composition was grown at temperatures much higher than 1200°C, and the equilibrium O_2 partial pressure becomes as high as 10 atm in this condition.

Our compositional analyses revealed that the Co content is less than the La content for $x \geqslant 0.5$. Then, the chemical formula is expressed as $Sr_{1-x}La_xFe_{12-y}Co_yO_{19}$. Suppose it has no defect, one formula unit contains y Co^{2+} and $(x - y)$ Fe^{2+} in addition to $(12 - x)$ Fe^{3+}. In order to obtain single crystals for $x \geqslant 0.5$, we grew single crystals that have the limited Co content of $y = 0.4$. In these compositions, we succeeded in growing single crystals. One of the cleaved surfaces is displayed in the right inset of Fig. 1, a clean surface of which indicates the absence of impurities. Chemical analysis using ICP shows that the La and Co contents of these single crystals are almost the same as the nominal compositions as shown in Fig. 1.

As mentioned above, we succeeded in obtaining single crystals of $Sr_{1-x}La_xFe_{12-y}Co_yO_{12}$ where $y = x$ for $x \leqslant 0.4$, and $y = 0.4$ for $x \geqslant 0.4$, under a 10 atm O_2 atmosphere. These single crystals, which have a variety of chemical compositions, exhibit systematic variation of the Curie temperature T_C as shown in the upper panel of Fig. 2, which indicates the success of single-crystal growth with a variety of chemical compositions. Although T_C monotonically decreases with x, the slope of the T_C-x curve differs below and above $x = 0.4$. For $x \leqslant 0.4$, T_C is suppressed by both La and Co substitutions with the slope of $dT_C/dx \approx -77.4$ K, which is consistent with a previous study [16]. For $x \geqslant 0.4$, T_C is suppressed by additional La substitution, and the slope is $dT_C/dx \approx -33.7$ K. The suppression of T_C in La- and Co-substituted samples with $x \leqslant 0.4$ is due to the reduction of exchange coupling in the network of magnetic ions, where a fraction of Fe^{3+} ions is replaced by Co^{2+} ions. Similarly, the suppression of T_C for $x \geqslant 0.4$ is caused by the replacement of Fe^{3+} with Fe^{2+}, the effect of which is suggested to be less than that of Co^{2+}. Another possible origin of the difference of the slope is that the substituted site depends on the amount of substitution.

Systematic variations are observed also in the lattice constants of the hexagonal unit cell. The variations of the lattice constants a and c; and the unit cell volume V are obtained by using powder x-ray diffraction as shown in the center and lower panels of Fig. 2, which is consistent with a previous study on powder samples [5]. As is different from T_C, we observed no difference between the slopes of curves below and above $x = 0.4$. This fact suggests that the difference between Co^{2+} and Fe^{2+} gives little influence. The value of a slightly increases with x, which is considered to be due to larger ionic radiuses of Co^{2+} and Fe^{2+} than that of Fe^{3+}. The difference of the ionic radii is approximately 0.1 Å [17]. At $x = 1$, the increment

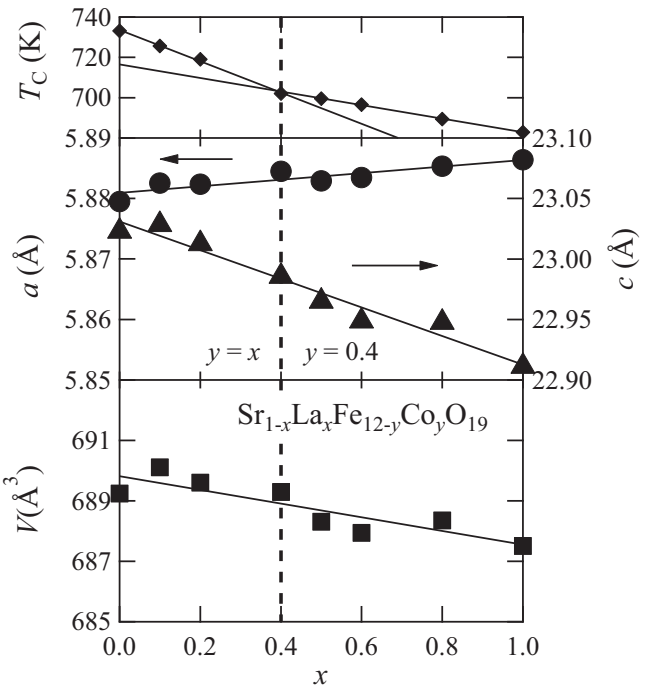

FIG. 2. The variations of T_C, the lattice constants and the unit cell volume of $Sr_{1-x}La_xFe_{12-y}Co_yO_{19}$ as a function of La content x. In the region of $x \leqslant 0.4$, the Co content y is equal to x. For $x \geqslant 0.4$, we fix $y = 0.4$. The lines in the graphs are the results of linear fittings.

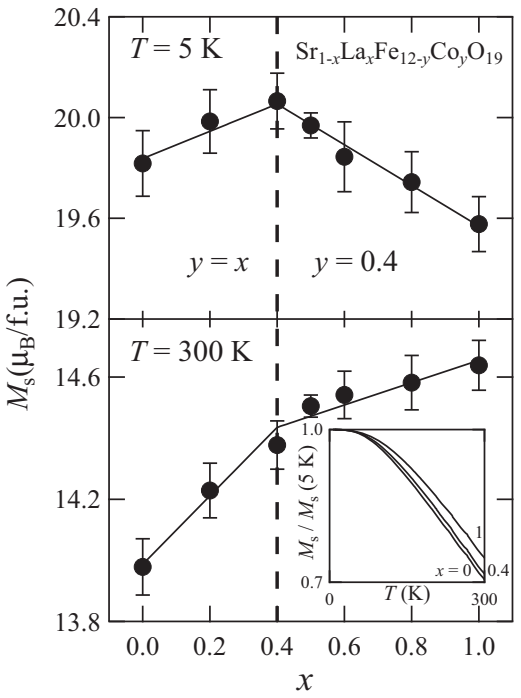

FIG. 3. The variation of saturation magnetization M_s per formula unit as a function of La content x. As is the same as before, the Co content y is equal to x for $x \leqslant 0.4$, and we fix $y = 0.4$ for $x \geqslant 0.4$. Upper and lower panels are the results measured at 5 and 300 K, respectively. The filled circles indicate the measured value and the bars scale experimental errors. The lines are guides to the eyes. The inset shows the temperature dependence of M_s for $x = 0, 0.4, 1$, which was measured at 1 T for $H \parallel c$.

of a reaches approximately 0.005 Å, which is 0.12% of a at $x = 0$. This increment is approximately one twentieth of the difference of the ionic radius. In contrast, the value of c substantially decreases with x, and the reduction of c at $x = 1$ is approximately 0.12 Å, which is 0.48% of c at $x = 0$. The decrement of c with x is mainly governed by La, which has a smaller ionic radius than that of Sr. These ions are coordinated by 12 oxygen atoms, and the difference of ionic radius with 12 coordination number is 0.08 Å [17]. Although one unit cell includes two La layers, the decrement of c is limited to one and half times as large as the difference of ionic radius. As a result of the variations of a and c, $V \propto a^2c$ decreases with x, and V at $x = 1$ is less than that at $x = 0$ by approximately 0.25%. If we ignore the difference of magnetization, this decrement of the volume enhances volume magnetization, which is preferable for permanent magnets.

Using these single crystals, we conducted systematic studies of magnetic properties. By applying a magnetic field H parallel to the c axis, which is easy axis, M easily saturates approximately at 0.1 T [13]. Thus saturation magnetizations M_s were obtained as shown in Fig. 3. Owing to the limit of the maximum range of the magnetometer we used, we have to use small single crystals, the typical mass of which is several milligrams. The experimental errors are evaluated to be approximately 1%, which are mainly due to both the resolution limit of the electric balance and the positional dependence of the sensitivity of the magnetometer. In spite of a margin of errors, systematic variation is clearly observed. At 5 K, M_s increases with x for $x \leqslant 0.4$ and decreases for $x \geqslant 0.4$. This result suggests a difference between the sites occupied by Co^{2+} for $x \leqslant 0.4$ and Fe^{2+} for $x \geqslant 0.4$. At $x = 0$, all the Fe ions are trivalent, having a d^5 electron configuration and a magnetic moment of $5\,\mu_B$, while Co^{2+} has an electron configuration of d^7 and a magnetic moment of $3\,\mu_B$. Suppose all the Co^{2+} occupy minority spin sites, increment of M_s at $x = 0.4$ should be $0.8\,\mu_B$. The observed increment is approximately half, which means that three fourth of Co^{2+} ions occupy minority spin sites, and the rest of them occupy majority spin sites. Our result is consistent with previous Mössbauer studies [7,8,18] that suggest Co^{2+} occupies the $2a$ (majority spin) site and the $4f_2$ (minority spin) site, and an NMR study [9] that suggests it occupies $4f_1$ (minority spin) or $4f_2$ sites. The difference between M_s at $x = 0.4$ and $x = 1$ is in good agreement with the value $0.6\,\mu_B$ calculated based on the assumption that all the Fe^{2+} ions with $4\,\mu_B$ occupy majority spin sites.

As is different from M_s at 5 K, M_s increases monotonically with x at 300 K, although the slope of M_s-x curve changes at $x = 0.4$. This difference arise from the temperature dependence of M_s. As shown in the inset of Fig. 3, M_s at $x = 1$ decreases slower than those at $x = 0, 0.4$ with increasing temperature. As a result, M_s at room temperature has the largest value at $x = 1$. The mean-field theory of ferrimagnets suggests that magnetization of small spin quantum number has smaller temperature dependence than that of large spin quantum number below T_C. Hence, considering that Fe^{2+} is placed in majority spin sites, thermal demagnetization would be suppressed

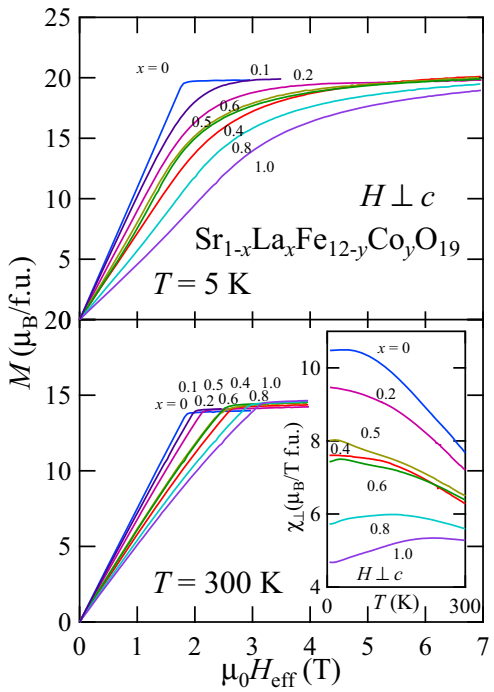

FIG. 4. The magnetization of $Sr_{1-x}La_xFe_{12-y}Co_yO_{19}$ where the magnetic field is applied perpendicular to the c axis. The effective magnetic field $H_{\rm eff}$ is obtained by subtracting the demagnetization field. The upper panel shows magnetization curves measured at 5 K, and the lower panel shows those at 300 K. The inset displays temperature dependence of magnetic susceptibility under magnetic field of 0.1 T in cooling process, which indicates the initial slopes of M-$\mu_0 H$ curves.

by the substitution of Fe^{3+} with Fe^{2+}, which has a smaller spin quantum number. Our experimental result is in good agreement with this explanation, while M_s at $x = 0$ and 0.4 have almost the same temperature dependence. The effect of small spin for the $x = 0.4$ sample is seemingly canceled, since Co^{2+} is distributed to both majority and minority spin sites.

In addition to the saturation magnetization, the magnetic anisotropy is one of the most important properties for materials for permanent magnet. Using single crystals, we can examine the magnetic anisotropy in detail. If a magnetic field is applied along the c axis of a single crystal, M steeply increases up to M_s owing to the strong easy axis magnetic anisotropy. This property was used in order to measure M_s. In contrast, if a magnetic field is applied perpendicular to the c axis of a single crystal, M gradually increases. In this case, the slope of the M-$\mu_0 H$ curve provides a measure of magnetic anisotropy.

The M-$\mu_0 H$ curves measured under H perpendicular to the c axis, are displayed in Fig. 4. At 300 K, all the M-$\mu_0 H$ curves are almost linear up to M_s, and show saturated behavior after that. The initial slope decreases with x, indicating increment of magnetic anisotropy both below and above $x = 0.4$. Similarly, the initial slope of M-$\mu_0 H$ curve measured at 5 K, seems to decrease with x. However, the M-$\mu_0 H$ curve measured at 5 K is qualitatively different from those at 300 K. Only for $SrFe_{12}O_{19}$ ($x = 0$), the curve is linear up to M_s as is the same as those at 300 K. For $x \geqslant 0.1$, M linearly increases with $\mu_0 H$ up to approximately 80% of M_s, and the slope gradually decreases. For largely substituted samples, M does not saturate even at 7 T, which is the highest field we applied. The decrement of the slope is possibly due to the effect of Co^{2+} or Fe^{2+}, which will be discussed later.

The value of H at which M reaches M_s is called anisotropy field H_A, which is a measure of magnetocrystalline anisotropy. At 300 K, each magnetization curve has a singular point. By using singular point detection technique, [19] H_A is defined as the value of H at the singular point, which is denoted as $H_{\rm SPD}$ here. At 300 K, the values of $\mu_0 H_{\rm SPD}$ can be easily evaluated from M-$\mu_0 H$ curves in the lower panel of Fig. 4. However, this technique does not work well at 5 K, since some of the magnetization curves at 5 K have no singular point. If a M-$\mu_0 H$ curve is a straight line up to M_s, H_A is expressed as $\mu_0 H_A = M_s/\chi_\perp$, where $\chi_\perp$ is $M/\mu_0 H$ under weak H that is applied perpendicular to the c axis. Here, we define H_A as $\mu_0 H_A = M_s/\chi_\perp(0.1\ {\rm T})$. Although the values of H_A at 300 K are slightly lower than those of $H_{\rm SPD}$, H_A can be measured in the entire temperature range by using this definition.

In order to obtain the temperature dependence of H_A, we measured the temperature dependence of M under 0.1 T, which is applied perpendicular to the c axis. As shown in the inset of Fig. 4, $\chi_\perp$ of the sample at $x = 0$ monotonically decreases with increasing temperature, the behavior of which is very similar to that of M_s in the inset of Fig. 3. In contrast, $\chi_\perp$ of the sample at $x = 1$ slightly increases with temperature. Using $\chi_\perp(T)$ under 0.1 T and $M_s(T)$, we calculated $\mu_0 H_A$ as a function of temperature, the result of which is shown in the inset of Fig. 5. At $x = 0$, $\mu_0 H_A$ ($\simeq \mu_0 H_{\rm SPD}$) is approximately equal to 1.8 T, which is almost independent of temperature. This value of H_A is consistent with a previous report [20]. With increasing x, H_A is highly enhanced at low temperatures. It reaches 4.2 T for the $x = 1$ sample at 5 K. However, H_A of high-x samples substantially decreases with increasing temperature. At 300 K, $\mu_0 H_A$ of the $x = 1$ sample is limited to 2.8 T, and $\mu_0 H_{\rm SPD}$ is approximately 3.0 T. Although this value is the highest value among previously reported M-type ferrites at room temperature, it is much lower than that at 5 K. The enhancement of $H_{\rm SPD}$ for $x \leqslant 0.4$ [18,20] and temperature dependence of $H_{\rm SPD}$ above 150 K [20,21] were already reported. Although H_A is slightly higher than $H_{\rm SPD}$ owing to the difference of definition, our results are consistent with previous reports. In contrast, the enhancement for $x \geqslant 0.4$ indicates that Fe^{2+} also enhances the magnetic anisotropy. Although the enhancement of H_A was reported for $LaFe_{12}O_{19}$ at low temperature [22], the enhancement for $x > 0.4$ at room temperature has not been reported before and discovered for the first time. Please recall that the Co content is fixed to 0.4 for $x \geqslant 0.4$.

To elucidate the origin of enhancement of H_A and gradual decrement of the slopes of M-$\mu_0 H$ curves at 5 K, we evaluated the magnetocrystalline anisotropy energy E_a. Using a M-$\mu_0 H$ curve under H perpendicular to the c axis, E_a can be obtained by

$$E_a(\theta) = \int_0^{M_s \sin\theta} \mu_0 H dM,$$

where θ is the angle between the c axis and the magnetization vector, namely, $\sin\theta = M/M_s$. If a M-$\mu_0 H$ curve is a straight

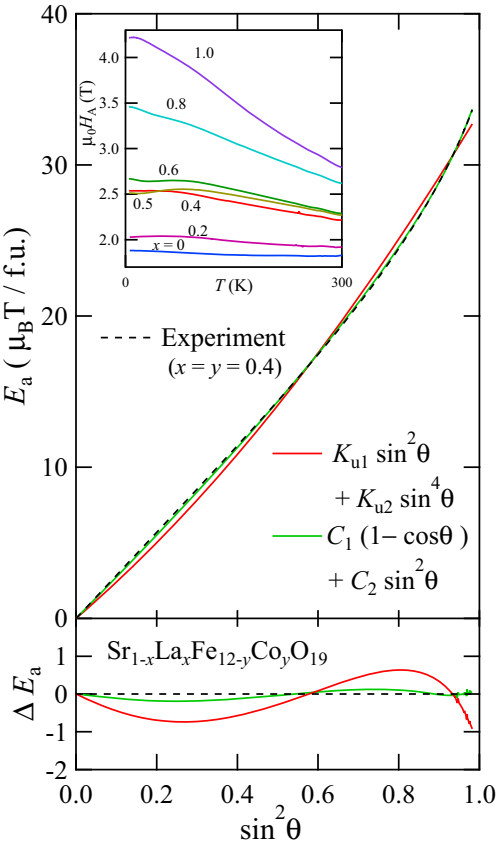

FIG. 5. The main panel shows the angle dependence of the magnetocrystalline anisotropy energy E_a of the $x = y = 0.4$ sample, $Sr_{0.6}La_{0.4}Fe_{11.6}Co_{0.4}O_{19}$. The experimentally obtained E_a- $\sin^2\theta$ curve, which displayed as a dashed line, is fitted using two formulas that are described in the figure. The lower panel shows the difference between experimental data and fitted ones. The inset displays the temperature dependence of $\mu_0 H_A$.

line and M saturates at $\mu_0 H = \mu_0 H_A$, E_a is expressed as $K_{u1} \sin^2\theta$, where $K_{u1} = \frac{1}{2} H_A M_s$ is the first uniaxial anisotropy constant. However, most of M-$\mu_0 H$ curves measured at 5 K is not linear, indicating that E_a is not expressed using above formula. In Fig. 5, E_a at 5 K for the $x = y = 0.4$ sample is plotted as a function of $\sin^2\theta$. The E_a- $\sin^2\theta$ curve is not linear, rather it is concave upward. We tried to fit this curve using the formula that includes higher-order terms [23],

$$E_a(\theta) = K_{u1} \sin^2\theta + K_{u2} \sin^4\theta + \cdots .$$

The curve using K_{u1} and K_{u2} is plotted in Fig. 5 as an example. Although the result is better than that using a line, it does not reproduce the rapid increase of experimentally obtained E_a around $\sin^2\theta = 1$. In order to reproduce it, very high-order terms are required. The introduction of very high-order term is not reasonable.

It was proposed that uniaxial magnetocrystalline anisotropy is enhanced by single ion anisotropy of Co^{2+}[24], which originates in spin-orbit interaction. The energy of spin-orbit interaction is given by $\lambda L \cdot S$, where λ is the spin-orbit coupling constant, and L is the nonvanishing orbital momentum. The direction of L is governed by crystal field, which depends on the sites. In the hexagonal M-type ferrite, the sum of L is

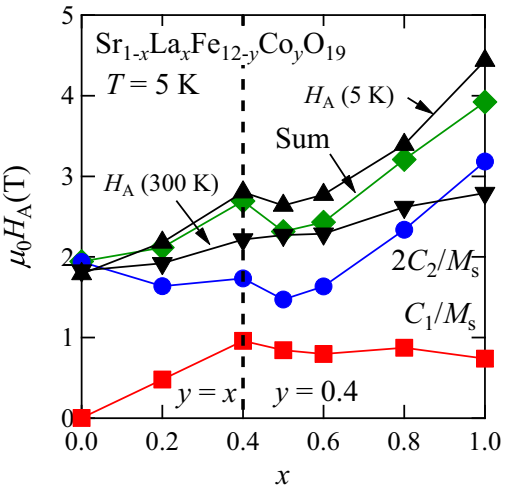

FIG. 6. The variations of two terms $2C_2/M_s$ and C_1/M_s and the sum of them, which were obtained from the fittings of E_a at 5 K. This figure includes also $\mu_0 H_A = M_s/\chi(0.1\ \mathrm{T})$ at 5 and 300 K.

considered to be parallel to the six fold axis, namely, the c axis. Hence we suppose $\lambda L \cdot S \propto \cos\theta$. In order to fit the E_a data, we used a formula including spin-orbit interaction,

$$E_a(\theta) = C_1(1 - \cos\theta) + C_2 \sin^2\theta,$$

where C_1 and C_2 are coefficients. The result of the fitting for the $x = y = 0.4$ sample is plotted in Fig. 5. Compared with the previous fitting, it well reproduce the data in all θ region, indicating that this formula is useful in this system.

In the Maclaurin series expansion of this formula as a function of $\sin\theta$, the coefficient of $\sin^2\theta$ is equal to $\frac{1}{2}C_1 + C_2$, which corresponds to K_{u1}. Using this coefficient, $\mu_0 H_A$ is given by $2K_{u1}/M_s = C_1/M_s + 2C_2/M_s$. In Fig. 6, C_1/M_s and $2C_2/M_s$ are plotted as a function of x, together with the sum of them and previously obtained $\mu_0 H_A = M_s/\chi(0.1\ \mathrm{T})$ at 5 K and 300 K in the inset of Fig. 5. The values of the sum of two terms are approximately equals to those obtained from $\chi(0.1\ \mathrm{T})$ at 5 K. For $x \leqslant 0.4$, the first term is proportional to $x = y$, which equals the concentration of Co^{2+}. It is nearly constant for $x \geqslant 0.4$, where y is fixed to the value 0.4. It is quite reasonable that the first term, which corresponds to spin-orbit interaction, is proportional to the content of Co^{2+}. In contrast, the second term is almost constant for $x \leqslant 0.6$, and increases with x after that. This increment for $x \geqslant 0.6$ is attributed to the effect of Fe^{2+}. As is the same as Co^{2+}, Fe^{2+} has nonvanishing orbital momentum and spin-orbit interaction. However, the details are different. The spin state of Fe^{2+} is usually treated as a fictitious spin $s = 1$ with the single ion anisotropy Ds_z^2 [25], which is likely to give $\sin^2\theta$ contribution to E_a. In the region of $0.4 \leqslant x \leqslant 0.6$, the Fe^{2+} has little effect on both the first and second terms. For $x \geqslant 0.6$, Fe^{2+} seemingly starts to occupy a certain site that has large D.

As previously mentioned, H_A is nearly independent of temperature for $x \leqslant 0.6$, and largely depends on temperature for $x > 0.6$. This difference is considered to be due to the difference between spin-orbit interactions of Co^{2+} and Fe^{2+}. The value of λ/k_B is reported to be approximately -256 and -148 K for Co^{2+} and Fe^{2+}, respectively [26]. At 300 K, the

spin-orbit interaction of Fe^{2+} is likely to be highly suppressed by thermal fluctuation owing to the small λ. In addition, the effect of Co^{2+} is also dependent on temperature in a different manner. At low temperatures, Co^{2+} has a spin state that is treated as a fictitious spin $s = 1/2$ as a result of spin-orbit interactions, and the single ion anisotropy of Co^{2+} is expressed as $\lambda L \cdot S$. With increasing temperature, the upper levels start to admix into the ground state, which violates the $s = 1/2$ state. As a result, the single ion anisotropy of Co^{2+} is in the form of Ds_z^2 at high temperatures. Hence the $\cos\theta$ term reduces and the M-$\mu_0 H$ curve becomes almost linear at room temperature, and the value of H_A is almost independent of temperature for $x \leqslant 0.6$, where the effect of Co^{2+} is dominant.

IV. CONCLUSIONS

In this work, we successfully grew single crystals of hexaferrites $Sr_{1-x}La_xFe_{12-y}Co_yO_{19}$ ($x = y$ for $x \leqslant 0.4$, $y = 0.4$ for $x \geqslant 0.4$), and investigated their magnetic properties. With increasing x, the unit cell volume decreases, and both saturation magnetization and anisotropy field monotonically increase. We conclude that $LaFe_{11.6}Co_{0.4}O_{12}$ is the best candidate that could have high maximum energy product in hexaferrites. Especially, by using the directly measured magnetic anisotropy of single crystals, we established a proper analysis method to characterize their microscopic origins. This analysis gives strong evidence that the enhancement of anisotropy field for $x \leqslant 0.4$ originates in the spin-orbit coupling of substituted Co^{2+} ions. Moreover, we found for the first time that the single ion anisotropy of Fe^{2+} also enhances the anisotropy field for $x \geqslant 0.4$ at room temperature. In this work, $LaFe_{11.6}Co_{0.4}O_{12}$ was prepared with the new idea that the same amount substitution of La and Co is not necessary for $Sr_{1-x}La_xFe_{12-y}Co_yO_{19}$ system, and that the produced Fe^{2+} further enhances magnetic properties. Our result indicates a possibility of developing a high H_A hexaferrite without Co utilizing the enhancement of H_A by Fe^{2+}.

ACKNOWLEDGMENTS

We thank H. Nakamura, Y. Tabata and T. Waki for helpful discussions, and K. Kazumi and N. Sasaki for SEM-WDX analysis, and S. Koike for ICP-AES measurement, which was carried out by the joint research in the Institute for Solid State Physics, the University of Tokyo. This work was supported by the Japan Science and Technology Agency (JST) under Collaborative Research Based on Industrial Demand "High Performance Magnets: Towards Innovative Development of Next Generation Magnets" (Grants No. 11103672 and No. 14532720).

[1] V. Adelsköld, Arkiv. Kemi. Min. Geol. **12A**, 1 (1938).
[2] J. J. Went, G. W. Rathenau, E. W. Gorter, and G. W. van Osterhout, Philips Tech. Rev. **13**, 194 (1952).
[3] A. Aharoni and M. Schieber, Phys. Rev. **123**, 807 (1961).
[4] A. H. Mones and E. Banks, J. Phys. Chem. Solids **4**, 217 (1958).
[5] K. Iida, Y. Minachi, K. Masuzawa, M. Kawakami, H. Nishio, and H. Taguchi, J. Magn. Soc. Jpn. **23**, 1093 (1999).
[6] P. B. Braun, Philos. Res. Rep. **12**, 491 (1957).
[7] J. M. Le Breton, J. Teillet, G. Wiesinger, A. Morel, F. Kools, and P. Tenaud, IEEE Trans. Mag. **38**, 2952 (2002).
[8] A. Morel, J. M. Le Breton, J. Kreisel, G. Wiesinger, F. Kools, and P. Tenaud, J. Magn. Magn. Mater. **242**, 1405 (2002).
[9] M. W. Pieper, F. Kools, and A. Morel, Phys. Rev. B **65**, 184402 (2002).
[10] Y. Kobayashi, E. Oda, T. Nishiuchi, and T. Nakagawa, J. Ceram. Soc. Jpn. **119**, 285 (2011).
[11] A. Balbashov and S. Egorov, J. Cryst. Growth **52**, 498 (1981).
[12] R. Gambino and F. Leonhard, J. Am. Ceram. Soc. **44**, 211 (1961).
[13] A. Shimoda, K. Takao, K. Uji, T. Waki, Y. Tabata, and H. Nakamura, J. Solid State Comm. **239**, 153 (2016).
[14] A. Aharoni, J. Appl. Phys. **83**, 3432 (1998).
[15] H. Morishita, A. Amano, H. Ueda, C. Michioka, and K. Yoshimura, J. Jpn. Soc. Powder Powder Metall. **61**, S64 (2014).
[16] H. Nishio, Y. Minachi, and H. Yamamoto, IEEE Trans. Magn. **45**, 5281 (2009).
[17] R. D. Shannon, Acta Cryst. A **32**, 751 (1976).
[18] P. Tenaud, A. Morel, F. Kools, J. M. Le Breton and L. Lechevallier, J. Alloys Compd. **370**, 331 (2004).
[19] G. Asti and S. Rinaldi, Phys. Rev. Lett. **28**, 1584 (1972).
[20] R. Grössinger, C. T. Blanco, M. Küpferling, M. Müller, and G. Wiesinger, Physica B **327**, 202 (2003).
[21] G. Asti, F. Bolzoni, J. M. Le Breton, M. Ghidini, A. Morel, M. Solzi, F. Kools, and P. Tenaud, J. Magn. Magn. Mater. **272**, E1845 (2004).
[22] M. Küpferling, R. Grössinger, M. W. Pieper, G. Wiesinger, H. Michor, C. Ritter, and F. Kubel, Phys. Rev. B **73**, 144408 (2006).
[23] R. F. Pearson, *Experimental Magnetism* (Wiley, New York, 1979).
[24] D. Alders, R. Coehoorn, and W. J. M. de Jonge, Phys. Rev. B **63**, 054407 (2001).
[25] K. Inomata and T. Oguchi, J. Phys. Soc. Jpn. **23**, 765 (1967).
[26] B. N. Figgis, *Introduction to Ligand Fields* (John Wiley & Sons Ltd., New York, 1966).